J|A|C|S
ARTICLES
Published on Web 04/17/2002

Structural Investigations into the *retro*-Diels-Alder Reaction. Experimental and Theoretical Studies

David Birney,*,† Tang Kuan Lim,‡ Joanne H. P. Koh,‡ Brett R. Pool,‡ and Jonathan M. White*,‡

Contribution from the School of Chemistry, University of Melbourne, Parkville, Vic 3010, Australia, and Texas Tech University, Lubbock, Texas 79409-1061

Received January 18, 2002

Abstract: The manifestations of the *retro*-Diels Alder reaction in the ground-state structures of a range of cyclopentadiene and cyclohexadiene cycloadducts **9**−**15** have been investigated by a combination of techniques. These include low-temperature X-ray crystallography, density functional calculations (B3LYP/6-31G(d,p)) on both the ground states and transition states, and the measurement of $^{13}C-^{13}C$ coupling constants. We have found that the carbon−carbon bonds (labeled bonds *a* and *b*), which break in the rDA, are longer in the cycloadducts **9**−**15** than in their corresponding saturated analogues **9s**−**15s**, which cannot undergo the rDA reaction. The degree of carbon−carbon bond lengthening appears to be related to the reactivity of the cycloadduct, thus the more reactive benzoquinone cycloadducts **5b** and **13** have longer carbon−carbon bonds. Those cycloadducts **14** and **15** which are predicted to undergo asynchronous reactions show differing degrees of carbon−carbon bond lengthening, reflecting the differing degrees of bond breaking at the calculated transition states for the rDA.

Introduction

In a recent communication we reported that crystal structures of cyclohexenes constrained into the boat conformation showed structural deformations consistent with the early stages of the *retro*-Diels-Alder reaction (rDA).[1] For example, an examination of the Cambridge Structural Database (CSD)[2] for those structures containing the bicyclo[2.2.1] moiety **1** showed that the bonds labeled *a* and *b*, which are broken in the *retro*-Diels-Alder reaction (Scheme 1), were on average 0.02 Å longer than

Scheme 1

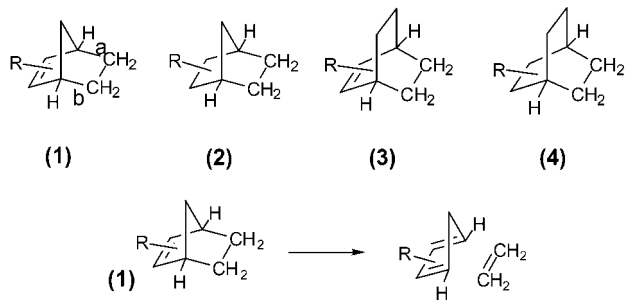

those in the corresponding saturated derivatives **2**. Similar, but smaller effects were also observed in the bicyclo[2.2.2]octenes **3** where the corresponding bonds were lengthened by only 0.009 Å relative to the saturated analogues **4**.

In the low-temperature crystal structure of the labile benzoquinone−cyclopentadiene cycloadduct **5**, we observed lengthening of 0.029 Å relative to the saturated derivative **6**. Vogel et

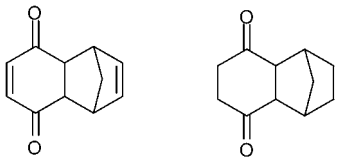

al.[3] measured the one-bond $^{13}C-^{13}C$ scalar coupling constants in a series of strained bicyclic alkanes and alkenes and found systematic differences in the magnitudes of these coupling constants between the saturated and unsaturated derivatives. An empirical relationship between carbon−carbon bond distance and the magnitude of the one-bond $^{13}C-^{13}C$ scalar coupling constants has been established,[4] and on this basis Vogel interpreted his results as implying contributions of the resonance form **7** (Scheme 2) to the ground state structure of the

Scheme 2

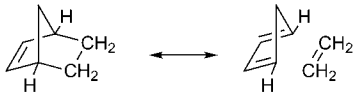

unsaturated derivatives. Significantly, no such effect was observed in monocyclic molecules which presumably do not favor the boat conformation.

* Corresponding author. E-mail: j.white@chemistry.unimelb.edu.au.
† Texas Tech University.
‡ University of Melbourne.

(1) Pool, B. R.; White, J. M. *Org. Lett*. **2000**, *2*, 3505−3507.
(2) Allen, F. H.; Bellard, S.; Brice, M. D.; Cartwright, B. A.; Doubleday: A.; Higgs, H.; Hummelink, T.; Hummelink-Peters, T.; Kennard, O.; Motherwell, W. D. S.; Rogers, J. R.; Watson, D. G. *Acta Crystallogr*. **1979**, *B35*, 2331
(3) Jones, G. R.; Caldarelli, S.; Vogel, P. *Helv. Chim. Acta* **1997**, *80*, 59.
(4) Unkefer, C. J.; London, R. E.; Whaley, T. W.; Daub, G. H. *J. Am. Chem. Soc*. **1983**, *105*, 733.

This is an example of the Structure Correlation Principle[5,6] in which structural changes associated with a chemical reaction can be manifested in the ground-state structure of the reactant as deviations of bond distances and angles from "normal values" along the reaction coordinate. Hence, bonds *a* and *b* which are broken in the *retro*-Diels-Alder reaction are lengthened in the ground state. The Structure Correlation Principle applies to molecules which exist in the ground state in a geometry that is similar to the transition state geometry for the reaction, hence an examination of the CSD for those cyclohexenes **8** which are not constrained to the boat conformation (and hence likely to exist in the generally preferred half-chair conformation) reveals "more normal" C−C bond distances of 1.520(4) Å,[7] this is also in accord with the observations of Vogel (above) on monocyclic alkenes. These structural effects presumably arise because the atomic and molecular orbitals whose interaction facilitates the reaction can also mix in the ground state. In the case of the *retro*-Diels-Alder reaction we have suggested that lengthening of bonds *a* and *b* results from interaction between the π orbital of the double bond and the σ^* orbitals of bonds *a* and *b*, and between the σ orbitals of bonds *a* and *b* bonds with the π^* orbital of the CC double bond.[1] These are the orbitals which interact during the *retro*-Diels-Alder reaction. In this paper we explore further the ground-state manifestations of the *retro*-Diels-Alder reaction in substituted cyclohexane derivatives constrained to the boat conformation, with the aim to establish (i) whether the degree of lengthening of the bonds *a* and *b* in the ground state relates to the ease at which the cyclohexane undergoes the *retro*-Diels-Alder reaction in solution or the gas phase and (ii) what types of structural effects arise in unsymmetrical cycloadducts. To this end we report here the results of our structural investigations on a range of Diels-Alder cycloadducts **9**−**15**, and their corresponding saturated analogues **9s**−**13s**, using low-temperature X-ray crystallography, NMR spectroscopy, and DFT calculations.

Results and Discussion

Synthesis. Compounds **9**−**13** were readily prepared by combining cyclopentadiene or cyclohexadiene with the appropriate dienophile in dichloromethane; the cycloadducts all had the expected endo geometry. Reduction to the saturated derivatives **9s**−**13s** was achieved in good yield by catalytic hydrogenation. The unsymmetrical adducts **14** and **16** were prepared by reaction of a 1:1 mixture of 1-trimethylsiloxycyclohexadiene and 2-trimethylsiloxycyclohexadiene with benzoquinone followed by chromatographic separation of the mixture of cycloadducts **14** and **16**, while **15** was prepared by reaction of 1-methoxycyclohexadiene with benzoquinone.

Molecular Structures. The X-ray crystal structures of compounds **9**−**15** and **12s** were determined at 130 K to minimize the unwanted effects of thermal motion. Details of the data collection and refinement for compounds **9**−**16** and **12s** are presented in Table 1, selected bond distances, angles, and dihedral angles are presented in Table 2, while bond distances which have been corrected for libration[8] are presented in Table 3. Crystals of the 1,3-cyclohexadiene−benzoquinone cycloadduct **13** were obtained in pure form in addition to mixed crystals of the cycloadduct in the presence of benzoquinone in the ratio 2:1 (**13.Q**); both these structures were determined. Unfortunately, of the saturated analogues, only compound **12s** gave crystals of suitable quality for an accurate structural determination. With the exception of the unsymmetrical adducts **14** and **15**, all the structures have an approximate local plane of symmetry bisecting the molecule, and in the case of **12** the molecule lies on a crystallographically defined plane of symmetry. There is excellent agreement between bond distances related by the local mirror plane in all structures.

Chart 1

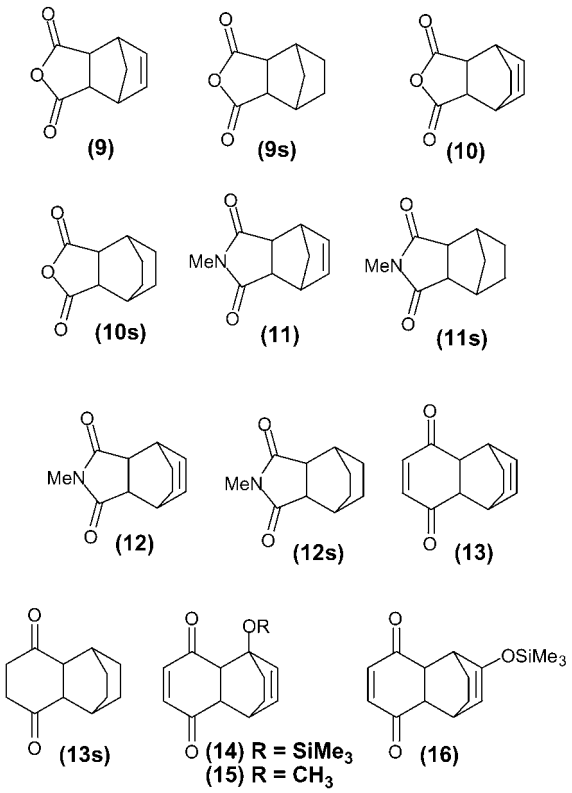

$^{13}C-^{13}C$ one bond scalar coupling constants for **9**−**12** and **9s**−**12s** were measured using the 1-D INADEQUATE experiment as previously reported.[9,10] Selected $^{13}C-^{13}C$ coupling constants for compounds **9**−**13** and **9s**−**13s** are presented in Tables 4 and 5. The magnitudes of the coupling constants correlate well with the observed and calculated bond distances in the expected sense.[3,4]

Computational Methods. All calculations were performed at the B3LYP/6-31G(d,p)[11] level using the Gaussian 94 and 98 suites of programs.[12] Geometries were fully optimized with no constraints. The nature of the stationary points was verified by frequency calculations; all transition structures had only one imaginary frequency that corresponded to the proposed reaction

(5) (a) Burgi, H. B.; Dunitz, J. D. *Acc. Chem. Res.* **1983**, *16*, 153. (b) Wipff, G.; Boudon, S. In *Accurate Molecular Structures*; IUCr Monographs on Crystallography 1, Oxford University Press: Oxford, 1992; Chapter 16.
(6) (a) Birney, D. M.; Wiberg, K. B.; Berson, J. A. *J. Am. Chem. Soc.* **1988**, *110*, 6631−6642. (b) Birney, D. M.; Ham, S.; Unruh, G. R. *J. Am. Chem. Soc.* **1997**, *119*, 4509−4517. (c) Birney, D. M. *J. Am. Chem. Soc.* **2000**, *122*, 10917−10925. (d) Shumway, W. W.; Dalley, N. K.; Birney, D. M. *J. Org. Chem.* **2001**, *66*, 5832−5839. (e) Jones, P. G.; Kirby, A. J. *J. Chem. Soc., Chem. Commun.* **1979**, 288−289.
(7) Allen, F. H.; Kennard, O.; Watson, D. G.; Brammer, L.; Orpen, A. G.; Taylor, R. *J. Chem. Soc., Perkin Trans. 2* **1987**, S1−S19.
(8) Trueblood, K. N.; Maverick, E. F. *THMA14c*, A TLS Thermal Motion Analysis based on experimentally measured anisotropic displacement parameters available from the WEB site: *www.chem.gla.ac.uk/*~louis/thma14/.
(9) Bax, A.; Freeman, R.; Kempsell, S. P. *J. Magn. Reson.* **1980**, *41*, 349.
(10) Bax, A.; Freeman, R.; Kempsell, S. P. *J. Am. Chem. Soc.* **1980**, *102*, 4849.

Table 1. Data Collection and Refinement Details for Compounds 9, 9s, and 10−15

compd no.	**9**	**10**	**11**	**12**	**13**	**13.Q**	**14**	**15**	**11s**
empirical formula	$C_9H_8O_3$	$C_{10}H_{10}O_3$	$C_{10}H_{11}NO_2$	$C_{11}H_{13}NO_2$	$C_{12}H_{12}O_2$	$C_{15}H_{14}O_3$	$C_{15}H_{20}O_3Si$	$C_{13}H_{14}O_3$	$C_{10}H_{13}NO_2$
formula wt	164.15	178.18	177.2	191.22	188.22	242.26	276.4	218.24	179.21
temp (K)	130.0(2)	130.0(2)	130.0(2)	130.0(2)	130.0(2)	130.0(2)	130.0(2)	130.0(2)	130.0(2)
radiation	Cu Kα	Cu Kα	Cu Kα	Cu Kα	Cu Kα	Cu Kα	Mo Kα	Cu Kα	Cu Kα
wavelength (Å)	1.5418	1.5418	1.5418	1.5418	1.5418	1.5418	0.71069	1.5418	1.5418
crystal system	orthorhombic	monoclinic	monoclinic	orthorhombic	orthorhombic	triclinic	monoclinic	orthorhombic	monoclinic
space group	$P2_12_12_1$	$P2_1/c$	$P2_1/c$	*Pnma*	$P2_12_12_1$	$P\bar{1}$	$P2_{1/n}$	*Pbca*	$P2_1/c$
unit cell dimens.									
a (Å)	5.9007(8)	6.514(1)	11.422(3)	12.177(2)	6.662(3)	6.716(4)	10.688(1)	7.762(3)	11.288(1)
b (Å)	9.455(2)	10.368(1)	6.284(3)	10.411(1)	11.647(5)	9.446(4)	12.460(2)	11.0450(6)	6.2158(3)
c (Å)	13.362(4)	12.060(1)	11.961(4)	7.626(10	12.397(1)	10.049(4)	11.768(2)	23.986(6)	12.746(1)
α (deg)						91.75(3)			
β (deg)		97.764(5)	98.38(3)			96.32(3)	112.24(1)		97.976(5)
γ (deg)						110.57(3)			
vol (Å^3)	745.5(3)	807.0(2)	849.4(5)	966.8(3)	961.9(6)	591.6(5)	1450.6(4)	2056.4(9)	885.7(1)
Z	4	4	4	4	4	2	4	8	4
D_c (g/cm^3)	1.463	1.466	1.386	1.314	1.3	1.36	1.266	1.41	1.344
m (mm^{-1})	0.926	0.901	0.795	0.736	0.705	0.77	0.163	0.813	0.763
F(000)	344	376	376	408	400	256	592	928	384
crystal size (mm)	0.5 × 0.4 × 0.2	0.5 × 0.3 × 0.2	0.4 × 0.3 × 0.2	0.5 × 0.5 × 0.15	0.5 × 0.2 × 0.15	0.5 × 0.4 × 0.4	0.6 × 0.4 × 0.4	0.5 × 0.5 × 0.4	0.6 × 0.3 × 0.2
θ range (deg)	5.73−74.85	5.65−74.78	3.91−74.04	6.85−74.91	5.21−74.79	4.44−69.93	2.20−25.02	6.79−74.93	3.95−75.00
index ranges	$-1 \le h \le 7$	$0 \le h \le 8$	$-14 \le h \le 14$	$-1 \le h \le 15$	$-8 \le h \le 1$	$0 \le h \le 8$	$0 \le h \le 12$	$0 \le h \le 9$	$0 \le h \le 14$
	$-1 \le k \le 11$	$0 \le k \le 12$	$-7 \le k \le 0$	$0 \le k \le 9$	$-14 \le k \le 1$		$-14 \le k \le 0$	$-13 \le k \le 0$	$0 \le k \le 7$
	$-1 \le l \le 16$	$-15 \le l \le 14$	$-14 \le l \le 14$	$0 \le l \le 13$	$-15 \le l \le 1$	$12 \le l \le 12$	$-13 \le l \le 12$	$0 \le l \le 30$	$-15 \le l \le 15$
no. of intensity controls	3	3	3	3	3	3	3	3	3
interval (min)	160	160	160	160	160	160	160	160	160
no. of reflcns collected	1304	1795	3050	1142	1621	2408	2698	2098	1909
no. of independent reflcns	1165	1652	1723	1046	1470	2222	2556	2098	1817
R_{int}	0.0362	0.0517	0.0197	0.0134	0.0187	0.0143	0.007	0	0.0205
completeness to *θ*	100%	100.00%	100.00%	99.80%	100.00%	99.10%	99.90%	99.50%	99.70%
no. of data/restraints/parameters	1165/0/142	1652/0/159	1723/0/163	1046/1/164	1470/0/176	2222/0/220	2556/0/253	2098/0/202	1817/0/171
goodness-of-fit on F^2	1.263	1.096	1.039	1.032	1.059	1.121	1.03	1.071	1.008
final *R* indices ($I > 2\sigma(I)$)	$R_{1\,=\,0.0429}$	$R_{1\,=\,0.0332}$	$R_{1\,=\,0.0372}$	$R_{1\,=\,0.0381}$	$R_{1\,=\,0.0332}$	R1 = 0.0397	$R_{1\,=\,0.0333}$	R1 = 0.0382	$R_{1\,=\,0.0364}$
	$wR_{2\,=\,0.0978}$	$wR_{2\,=\,0.0842}$	$wR_{2\,=\,0.0891}$	$wR_{2\,=\,0.1157}$	$wR_{2\,=\,0.0788}$	wR2 = 0.1040	$wR_{2\,=\,0.0839}$	$wR_{2\,=\,0.1034}$	$wR_{2\,=\,0.0988}$
R indices (all data)	$R_{1\,=\,0.0448}$	$R_{1\,=\,0.0356}$	$R_{1\,=\,0.0391}$	$R_{1\,=\,0.0417}$	$R_{1\,=\,0.0414}$	R1 = 0.0409	$R_{1\,=\,0.0396}$	$R_{1\,=\,0.0403}$	$R_{1\,=\,0.0397}$
	$wR_{2\,=\,0.0995}$	$wR_{2\,=\,0.0861}$	$wR_{2\,=\,0.0902}$	$wR_{2\,=\,0.1222}$	$wR_{2\,=\,0.0836}$	wR2 = 0.1051	$wR_{2\,=\,0.0885}$	$wR_{2\,=\,0.1048}$	$wR_{2\,=\,0.1030}$
weighting scheme:									
$w = 1/[\sigma^2(F_o^2) + (A^*P)^2 + B^*P]$,	$A = 0.0682$	$A = 0.0381$	$A = 0.0326$	$A = 0.0923$	$A = 0.0453$	A = 0.0458	$A = 0.0436$	$A = 0.0507$	$A = 0.0584$
where $P = (F_o^2 + 2F_c^2)/3$	$B = 0.0059$	$B = 0.3317$	$B = 0.5297$	$B = 0.2440$	$B = 0.1282$	B = 0.0723	$B = 0.7753$	$B = 1.3652$	$B = 0.3667$
extinction method	SHELXL	SHELXL	SHELXL	SHELXL	SHELXL	SHELXL	SHELXL	SHELXL	SHELXL
extinction coeff	0.088(6)	0.076(3)	0.028(1)	0.011(2)	0.0030(7)	0.0096(14)	0.006(1)	0.0111(6)	0.010(1)
largest diff. peak and hole (e·Å^{-3})	0.268, −0.319	0.292, −0.180	0.261, −0.189	0.315, −0.197	0.204, −0.137	0.274, −0.242	0.315, −0.344	0.280, −0.231	0.242, −0.179

Table 2. Selected Distances and Angles for Compounds **5**, **6**, **9**−**13**, and **15**

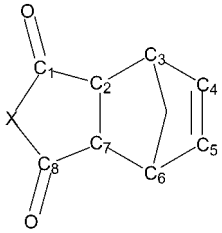

	5[a]	6[a]	9	10	11	12	13	13.Q	14	15	11s
C1−C2	1.501(2)	1.516(2)	1.498(2)	1.504(2)	1.507(2)	1.509(2)	1.506(3)	1.508(2)	1.509(2)	1.510(2)	1.506(2)
C2−C3	1.575(2)	1.553(2)	1.569(2)	1.549(2)	1.5706()	1.548(2)	1.566(2)	1.563(2)	1.581(2)	1.585 (2)	1.549(2)
C3−C4	1.507(2)	1.534(2)	1.520(3)	1.507(2)	1.515(19)	1.506(2)	1.499(3)	1.504(2)	1.499(2)	1.509(2)	1.538(2)
C4−C5	1.327(3)	1.553(2)	1.323(3)	1.329(2)	1.327(2)	1.327(3)	1.323(3)	1.328(2)	1.324(2)	1.328(2)	1.556(2)
C5−C6	1.512(2)	1.544(2)	1.518(3)	1.508(2)	1.517(2)	1.506(2)	1.495(3)	1.503(2)	1.503(2)	1.506(2)	1.537(2)
C6−C7	1.571(2)	1.537(2)	1.570(2)	1.550 (2)	1.570(2)	1.548(2)	1.565(3)	1.558(2)	1.559(2)	1.554(2)	1.547(2)
C7−C8	1.503(2)	1.510(2)	1.499(3)	1.503(2)	1.502(2)	1.509(2)	1.512(2)	1.517(2)	1.511(2)	1.519(2)	1.506(2)
C1−O1	1.224(2)	1.217(2)	1.188(2)	1.192(2)	1.216(2)	1.211(1)	1.218(2)	1.222(2)	1.221(2)	1.218(2)	1.214(2)
C8−O2	1.222(2)	1.216(2)	1.194(2)	1.194(2)	1.210(2)	1.211(1)	1.217(2)	1.223(2)	1.221(2)	1.222(2)	1.215(2)
C2−C3−C4	106.3(2)	109.1(1)	106.4(1)	108.1(1)	106.1(1)	108.4(1)	107.2(2)	108.34(11)	108.9(1)	110.2(1)	109.8(1)
C5−C6−C7	105.7(1)	109.4(1)	107.7(2)	108.0(1)	107.1(1)	107.3(3)	108.4(2)	107.08(12)	107.2(1)	106.2(1)	109.6(1)

[a] See ref 1.

Table 3. Bond Distances Corrected for Thermal Libration

	5	6	9	10	11	12	13	13.Q	14	15	11s
C1−C2	1.506	1.522	1.500	1.507	1.510	1.512	1.510	1.512	1.512	1.512	1.510
C2−C3	1.581	1.558	1.572	1.553	1.574	1.552	1.571	1.567	1.585	1.587	1.553
C3−C4	1.512	1.541	1.524	1.511	1.518	1.513	1.504	1.508	1.502	1.511	1.543
C4−C5	1.331	1.558	1.326	1.333	1.330	1.333	1.328	1.332	1.328	1.331	1.561
C5−C6	1.517	1.550	1.521	1.511	1.521	1.513	1.500	1.507	1.506	1.509	1.542
C6−C7	1.576	1.542	1.573	1.553	1.574	1.552	1.570	1.562	1.563	1.556	1.551
C7−C8	1.507	1.515	1.502	1.506	1.505	1.512	1.517	1.521	1.513	1.521	1.510
C1−O1	1.226	1.222	1.191	1.195	1.219	1.216	1.222	1.226	1.224	1.220	1.218
C8−O2	1.226	1.221	1.196	1.197	1.213	1.216	1.222	1.226	1.224	1.224	1.219

Table 4. $^{13}C-^{13}C$ One Bond Scalar Coupling Constants for Bonds *a* and *b* in Cycloadducts **9**−**12** and the Saturated Analogs **9s**−**12s**

		9s–**12s**	ΔJ (Hz)	ΔCC (Å) (obsd)	ΔCC (Å) (calcd)
9	27.5	30.8	3.3		0.02
10	30.5	31.7	1.2		0.01
11	28.1	31.7	3.6	0.022	0.021
12	31.1	32.4	1.3		0.011

Table 5. $^{13}C-^{13}C$ One-Bond Scalar Coupling Constants for Bonds between the Bridgehead Atoms and the Ethylene Bridges in Compounds **10**, **12**, **10s**, and **12s**

10	31.1
10s	32.81, 33.2
12	31.1
12s	32.74, 33.12

coordinate. Due to the flexibility of the molecules, some of the optimizations were completed with negligible forces, but with displacements slightly above the default cutoffs, as detailed in the Supporting Information. These geometries were accepted if the frequency calculation reported that the geometry was converged. The relevant bond distances are shown in Table 6. For selected structures the transition state structures were also calculated. These are shown in Figure 1 with relevant geometrical data in Table 7. The relative energies of isomeric compounds, energies of hydrogenation, and energies of reaction are summarized in Table 8. Relative energies include unscaled zero-point vibrational energy corrections. Optimized geometries and absolute energies are reported in the Supporting Information. For **15TS**, a natural bond orbital (NBO) analysis was performed.[13]

There is in general, excellent agreement between the calculated (Table 6) and observed bond distances (corrected for

(11) (a) Becke, A. D.; *J. Chem. Phys.* **1993**, *98*, 5648. (b) For the 6-31G basis set: Hariharan, P. C.; Pople, J. A. *Theor. Chim. Acta* **1973**, *28*, 213. (c) The reliability of the B3LYP/6-31G(d,p) method has been supported by numerous calculations. For leading references, see: McKee, M. L.; Shevlin, P. B.; Zottola, M. *J. Am. Chem. Soc.* **2001**, *123*, 9418, (d) Curtiss, L. A.; Raghavachari, K.; Redfern, P. C.; Pople, J. A. *J. Chem. Phys.* **1997**, *106*, 1063. (e) Singleton, D. A.; Merrigan, S. R.; Liu, J.; Houk, K. N. *J. Am. Chem. Soc.* **1997**, *119*, 3385. (f) Hrovat, D. A.; Chen, J.; Houk, K. N.; Borden, W. T. *J. Am. Chem. Soc.* **2000**, *122*, 7456. (g) Cossío, F. P.; Arrieta, A.; Lecea, B.; Alajarín, M.; Vidal, A.; Tovar, F. *J. Org. Chem.* **2000**, *65*, 3633. (h) Birney, D. M. *J. Am. Chem. Soc.* **2000**, *122*, 10917.

(12) (a) Frisch, M. J.; Trucks, G. W.; Schlegel, H. B.; Gill, P. M. W.; Johnson, B. G.; Robb, M. A.; Cheeseman, J. R.; Keith, T.; Petersson, G. A.; Montgomery, J. A.; Raghavachari, K.; Al-Laham, M. A.; Zakrzewski, V. G.; Ortiz, J. V.; Foresman, J. B.; Peng, C. Y.; Ayala, P. Y.; Chen, W.; Wong, M. W.; Andres, J. L.; Replogle, E. S.; Gomperts, R.; Martin, R. L.; Fox, D. J.; Binkley, J. S.; Defrees, D. J.; Baker, J.; Stewart, J. P.; Head-Gordon, M.; Gonzalez, C.; Pople, J. A. *Gaussian 94*, Revision B.3; Gaussian, Inc.: Pittsburgh, PA, 1995. (b) Frisch, M. J.; Trucks, G. W.; Schlegel, H. B.; Scuseria, G. E.; Robb, M. A.; Cheeseman, J. R.; Zakrzewski, V. G.; Montgomery, J. A., Jr.; Stratmann, R. E.; Burant, J. C.; Dapprich, S.; Millam, J. M.; Daniels, A. D.; Kudin, K. N.; Strain, M. C.; Farkas, O.; Tomasi, J.; Barone, V.; Cossi, M.; Cammi, R.; Mennucci, B.; Pomelli, C.; Adamo, C.; Clifford, S.; Ochterski, J.; Petersson, G. A.; Ayala, P. Y.; Cui, Q.; Morokuma, K.; Malick, D. K.; Rabuck, A. D.; Raghavachari, K.; Foresman, J. B.; Cioslowski, J.; Ortiz, J. V.; Stefanov, B. B.; Liu, G.; Liashenko, A.; Piskorz, P.; Komaromi, I.; Gomperts, R.; Martin, R. L.; Fox, D. J.; Keith, T.; Al-Laham, M. A.; Peng, C. Y.; Nanayakkara, A.; Gonzalez, C.; Challacombe, M.; Gill, P. M. W.; Johnson, B.; Chen, W.; Wong, M. W.; Andres, J. L.; Gonzalez, C.; Head-Gordon, M.; Replogle, E. S.; Pople, J. A. *Gaussian 98*, Rev. A.6 ed.; Gaussian, Inc.: Pittsburgh, PA, 1998.

(13) Weinhold, F.; Carpenter, J. E. *The Structure of Small Molecules and Ions*; Plenum: New York, 1988.

Table 6. Calculated Distances for Compounds 9−13, 15 and 9s-13s, 15s

	5	6	9	10	11	12	13	15	9s	10s	11s	12s	13s	15s
C1−C2	1.519	1.523	1.516	1.521	1.521	1.525	1.527	1.520	1.517	1.520	1.521	1.525	1.527	1.521
C2−C3	1.582	1.552	1.580	1.559	1.578	1.558	1.567	1.600	1.560	1.549	1.557	1.547	1.555	1.584
C3−C4	1.522	1.548	1.523	1.513	1.522	1.513	1.512	1.509	1.547	1.542	1.548	1.542	1.541	1.540
C4−C5	1.341	1.564	1.341	1.339	1.341	1.339	1.339	1.336	1.564	1.558	1.564	1.559	1.557	1.552
C5−C6	1.522	1.547	1.523	1.513	1.523	1.513	1.512	1.510	1.547	1.542	1.548	1.542	1.541	1.540
C6−C7	1.582	1.561	1.580	1.559	1.578	1.558	1.567	1.567	1.560	1.549	1.557	1.547	1.555	1.553
C7−C8	1.519	1.529	1.561	1.521	1.521	1.525	1.527	1.529	1.517	1.520	1.521	1.525	1.527	1.530
C1−O1	1.223	1.217	1.197	1.198	1.215	1.215	1.223	1.223	1.197	1.198	1.215	1.215	1.223	1.223
C8−O2	1.223	1.217	1.197	1.198	1.215	1.215	1.223	1.223	1.197	1.198	1.215	1.215	1.223	1.223
C2−C7	1.560	1.573	1.542	1.539	1.550	1.546	1.558	1.566	1.547	1.543	1.554	1.550	1.570	1.572
H2−C2−C7	110.0	109.3	114.4	113.0	113.8	112.5	109.0	108.7	114.0	112.5	113.4	112.0	108.7	108.6

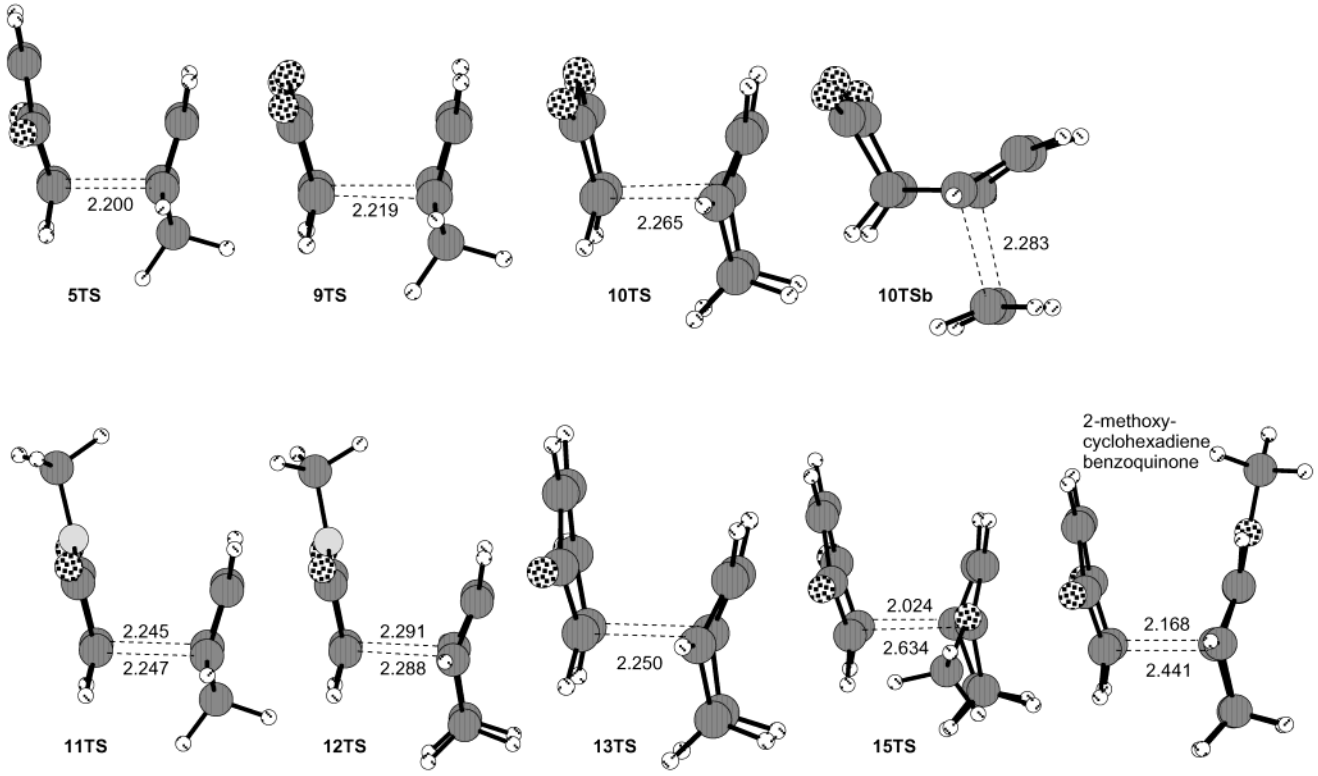

Figure 1.

Table 7. Transition State Geometries for *retro*-Diels-Alder Reaction of Compounds **5**, **9**−**13**, and **15**

	5TS	9TS	10TS	11TS	12TS	13TS	15TS
C1−C2	1.481	1.480	1.480	1.492	1.491	1.480	1.447
C2−C3	2.200	2.219	2.265	2.245	2.291	2.250	2.634
C3−C4	1.406	1.404	1.392	1.400	1.388	1.395	1.395
C4−C5	1.398	1.400	1.402	1.404	1.405	1.400	1.391
C5−C6	1.406	1.404	1.391	1.400	1.388	1.395	1.410
C6−C7	2.202	2.219	2.266	2.247	2.289	2.250	2.204
C7−C8	1.480	1.480	1.480	1.491	1.491	1.480	1.500
C1−O1	1.227	1.200	1.202	1.217	1.218	1.228	1.240
C8−O2	1.227	1.200	1.202	1.217	1.218	1.228	1.227

Table 8. Barrier Heights, Relative Energies, Energies of Hydrogenation, and Energies of Reaction (kcal/mol) (Calculated at the B3LYP/6-31G(d,p) + ZPE[a] Level)

	5	9	10	11	12	13	15
barrier[b]	27.0	30.3	43.6[c]	33.7	46.8	37.7	29.1
retro-D−A[d]	10.2	16.2	26.1	18.8	28.7	17.6	8.8
hydrogenation[e]	−30.8[f]	−31.2	−26.7	−31.2	−26.6	−26.5[f]	−26.7[f]

[a] Zero-point energy correction (unscaled). [b] Barrier height for *retro*-Diels-Alder fragmentation of compound. [c] Barrier for loss of ethene from **10** is 51.5 kcal/mol. [d] Overall change in energy for *retro*-Diels-Alder fragmentation of compound. [e] Hydrogenation energy for addition of H_2 to the C_4−C_5 π-bond. [f] Hydrogenation energies for the quinone π-bonds are 20.3 kcal/mol for **6** and 20.5 kcal/mol for both **13** and **15**.

libration, Table 3) for the cycloadducts **9**−**15** and the one saturated analogue **11s** for which good-quality X-ray data are available. This gives us confidence that the calculated structural parameters for the remaining saturated compounds **9s**−**10s** and **12s**−**13s** can be reliably used for comparison purposes. Inspection of the experimental and calculated data summarized in Tables 3 and 6 reveals that the *a* and *b* bond distances (labeled as C2−C3 and C6−C7, see labeling scheme Table 1) within the strained [221] bicyclic framework of the cyclopentadiene cycloadducts **5**, **9**, and **11** are consistently longer than the corresponding distances within the [222] bicyclic framework of the cyclohexadiene cycloadducts **10**, **12**, and **13** while the bonds C1−C2 and C7−C8 which are exocyclic to the bicyclic ring system are slightly shorter. This is in accord with conventional strain considerations, thus ring strain should shorten exocyclic bonds and lengthen bonds within the strained ring system.[14]

There are also some other consistent patterns in the geometries. The first is that the C2−C3 and C7−C8 bond lengths (bonds *a* and *b*) are consistently longer (generally 0.01 to 0.02 Å) in those molecules that can undergo a *retro*-Diels-Alder reactions compared to those that cannot. Tables 3 and 6 also reveal that the magnitude of these structural effects is larger in the cyclopentadiene cycloadducts than in the corresponding cyclohexadiene cycloadducts. For example, the C2−C3 and C7−C8 bond distances for the unsaturated cyclopentadiene cycloadducts **5**, **9**, and **11** are calculated to be 0.022, 0.020, and 0.021 Å, respectively, longer than the corresponding distances in the saturated derivatives **6**, **9s**, and **11s**. The observed difference between these bonds in **11** and **11s** was 0.022 Å, again showing an excellent agreement between theory and experiment. The corresponding differences calculated for the cyclohexadiene cycloadducts **13** and **13s**; **10** and **10s**; and **12** and **12s** were 0.012, 0.010, and 0.011 Å, respectively, and are clearly smaller. Similar conclusions are drawn by comparing the $^{13}C-^{13}C$ scalar coupling constants for these bonds in compounds **9**−**12** and **9s**−**12s**. Thus the differences in the $^{13}C-^{13}C$ scalar coupling constants for the cyclopentadiene cycloadducts **9** and **10** and the saturated analogues **9s** and **10s** were 3.3 and 3.6 Hz, respectively. By comparison the difference in the $^{13}C-^{13}C$ scalar coupling constants for the cyclohexadiene cycloadducts **10** and **12** and the saturated analogues **10s** and **12s** was only 1.2 and 1.1 Hz, respectively.

Similarly, the calculated C2−C7 bond distances are shorter in those molecules that can undergo the rDA reaction than in the saturated ones. For example, the C2−C7 distance is 0.005 Å shorter in **9** than in **9s**, and 0.012 Å shorter in **13** than in **13s**. Also, the H2−C2−C7 angle is more open in the molecules that can fragment, as C2 becomes more sp^2 hybridized, e.g. **9** (114.4°) as compared to **9s** (114.0°) and **13** (109.0°) as compared to **13s** (108.7°). These trends are consistent with more double bond character in those molecules where fragmentation is possible.

We offer three possible explanations for the larger structural effects observed in the cyclopentadiene cycloadducts as compared to the cyclohexadiene adducts. The first two explanations are based on the additional strain present in the norbornene (bicyclo[2.2.1]hept-2-ene) ring system that is relieved in the *retro*-Diels-Alder reaction. First, it can be argued that lengthening of the C2−C3 and C6−C7 bonds in both sets of cycloadducts arises from interaction between the σ and σ^* orbitals of these bonds with the π and π^* orbitals of the double bond. The greater angle strain could be postulated to raise the energy of the σ orbitals of the breaking *a* and *b* bonds (C2−C3 and C6−C7) in the 221 systems and similarly lower the energy of the σ^* orbitals.[15] In simple frontier orbital terms this would result in a stronger interaction between these σ orbitals with the π^* orbital and between the σ^* and π orbitals in the 221 systems compared with the 222 systems. Both of these effects would weaken and lengthen bonds *a* and *b*.

Table 9. Calculated Distances (Å) between the Bridgehead Carbons and the Ethano Bridge Carbons in Compounds **10**, **10s**, **12**, and **12s**

	C_b-CH_2
10	1.555
10s	1.543
12	1.555
12s	1.547

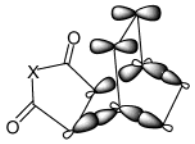

Figure 2.

A second possibility is that the additional ring strain of the 221 system directly manifests itself in longer endocyclic bonds and shorter exocyclic bonds. This trend is commonly observed in a wide range of strained systems and has been interpreted as a change toward higher π-character in the endocyclic bonds and higher σ-character in the exocyclic bonds.[16] The greater strain in the 221 systems is indirectly manifested in the calculated energy of hydrogenation. These energies are consistently more exothermic (4−5 kcal/mol) for the 221 systems than for the 222 system (see Table 8).

A third alternative explanation for the smaller structural effects observed in the [222]-alkenes arises upon examination of the bond distances between the bridgehead carbons and the ethano bridge carbons for **10** and **12**. Comparison of these bond distances with those in the saturated analogues **10s** and **12s** (Table 9) reveals these bonds are ca. 0.012 and 0.013 Å, respectively, longer in the unsaturated molecules; these are the bonds which break in the alternative *retro*-Diels-Alder reaction for loss of ethylene. In fact the degree of lengthening of the bonds to the ethylene bridge is slightly greater (than that for the bonds to the maleimide/anhydride moiety) and furthermore the $^{13}C-^{13}C$ coupling constants between the bridgehead carbons and the ethylene bridge increase by ca. 1.5−2.1 Hz upon saturation (Table 5). It is therefore interesting to note that closely related cyclohexadiene cycloadducts undergo loss of ethylene upon heating in sealed tubes.[17] Perhaps interaction of the π orbitals with two sets of σ orbitals (Figure 2) results in a dilution of the structural effects over the two sets of C−C σ bonds.

To further probe this particular question, we calculated the transition structures for the *retro*-Diels-Alder reactions for the loss of ethylene and for the loss of cyclohexadiene from **10**. The transition structure for loss of ethylene (**10TS2**) is only 7.9 kcal/mol higher in energy than that for the rDA for loss of cyclohexadiene via **10TS**. This result suggests that the Diels-Alder reaction between maleic anhydride and cyclohexadiene is reversible, but that the loss of ethylene is irreversible under these conditions.

Is there a relationship between the degree of lengthening of the bonds that break in the *retro*-Diels-Alder reaction and the reactivity of the cycloadduct toward this reaction? Our data

(14) (a) Wiberg, K. B.; Bader, R. F. W.; Lau, C. D. H. *J. Am. Chem. Soc.* **1897**, *109*, 1001. (b) Stanger, A. *J. Am. Chem. Soc.* **1998**, *120*. These effects have been recently utilized to stabilize planar cyclooctatetraenes. (c) Baldridge, K. K.; Siegel, J. S. *J. Am. Chem. Soc.* **2001**, *123*, 1755−1759. (d) Matsuura, A.; Komatsu, K. *J. Am. Chem. Soc.* **2001**, *123*, 1768.

(15) (a) Brown, R. S.; Traylor, T. G., *J. Am. Chem. Soc*. **1970**, *92*, 5228. (b) Streitwieser, A., Jr.; S. Alexandratos, *J. Am. Chem. Soc.* **1978**, *100*, 1979.

(16) Engler, E. M.; Andose, J. D.; Schleyer, P. v. R. *J. Am. Chem. Soc.* **1973**, *95*, 8005.

(17) (a) Hugo, V. I.; Nicholson, J. L.; Snijman, P. W. *Synth. Commun*. **1994**, *24*, 23. (b) Dimitriadis, C.; Gill, M.; Harte, M. F. *Tetrahedron Assym*. **1997**, *8*, 2153.

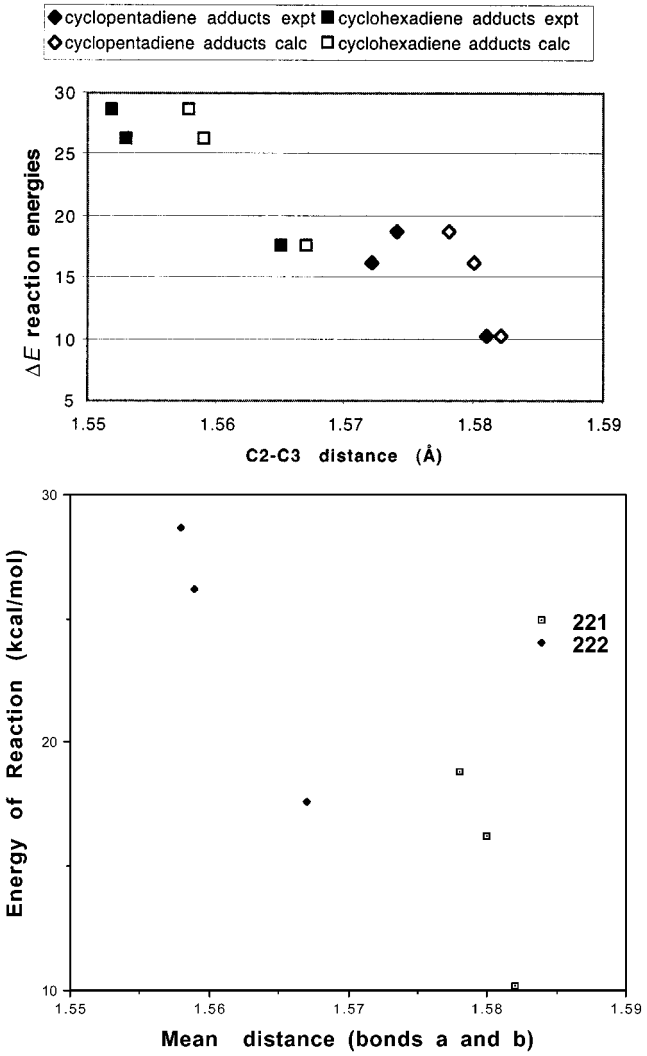

Figure 3. Experimental and calculated (B3LYP/6-31G(d,p)) bond distances vs calculated reaction energies (ΔE) for **5**, **9**, and **11** (cyclopentadiene adducts) and for **10**, **12**, and **13** (cyclohexadiene adducts). Data from Tables 3, 6, and 7. Note that the average experimental bond distances *a* and *b*, as well as the distances for **13Q**, were used.

provide qualitative and quantitative evidence that this is indeed the case within the cyclopentadiene and cyclohexadiene series. For example, as noted above, the more strained cyclopentadiene cycloadducts **5**, **9**, and **11** show lengthening of the C2−C3 and C7−C8 bonds by 0.02 Å compared with their saturated analogues, whereas the cyclohexadiene cycloadducts also show lengthening, although of only 0.01 Å. Furthermore, within these two series, the reactive benzoquinone cycloadducts both have longer C2−C3 and C6−C7 bonds than the less reactive *N*-methyl maleimide and maleic anhydride cycloadducts. To quantify this relationship, the changes in calculated energies for the *retro*-Diels-Alder reactions are plotted in Figure 3 versus both the experimental and the calculated *a* and *b* bond lengths for the cyclopentadiene adducts **5**, **9**, and **11** and separately for the cyclohexadiene adducts **13**, **10**, and **12**. We note that the calculated energies include the release of strain in the fragmentations. Although this is admittedly a limited data set, within each group, the longer bond lengths are consistently found for the easier *retro*-Diels-Alder reactions. This strongly supports the assertion that the bond lengths reflect the incipient *retro*-Diels-Alder reaction. The lack of correlation between the

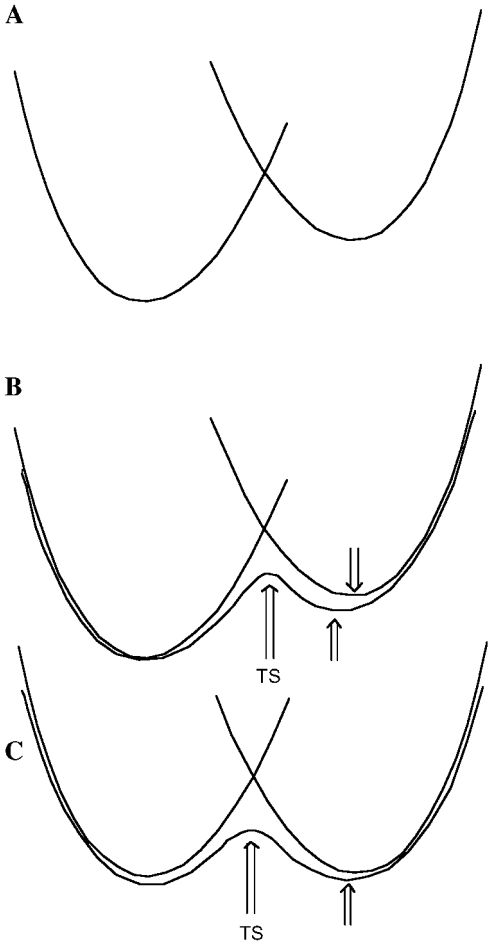

Figure 4. Schematic representation of potential energy surfaces according to the Bell−Evans−Polanyi principle.

cyclohexadiene and cyclopentadiene series supports the argument that the competing reaction for loss of ethylene in the cyclohexadiene series dilutes the structural effects for bonds *a* and *b*.

There is indeed a more fundamental relationship between the bond lengths of the ground-state molecules, the bond lengths in the transition structures, and the energetics of the reactions. This was first formulated as the Bell−Evans−Polanyi principle.[18] It can be most easily described by considering the potential energy surfaces of the reactants and products first as smooth, noninteracting curves, as in Figure 4A. The potential energy surface for the reaction is then obtained by allowing the two states to mix. If the degree of mixing is inversely proportional to the energy spacing between the states, then the potential energy surface for an endothermic reaction is as shown in Figure 4B and for a thermoneutral reaction it is as shown in Figure 4C. This very qualitative picture predicts all of the aspects of the *retro*-Diels-Alder reactions that have been described above. Specifically, (1) this description leads to the familiar Hammond postulate,[19] that the transition state for an endothermic reaction should resemble the products. This is the case; for the more endothermic fragmentations of maleic anhydride derivatives, the calculated transition states have the longest partial bonds (see Figure 1, and Table 7). (2) However, this qualitative

(18) Bell, R. P. *Proc. R. Soc. London, Ser. A* **1936**, *154*, 414. (b) Evans, M. G.; Polanyi, M. *Trans. Faraday. Soc.* **1938**, *34*, 11.
(19) Hammond, G. S. J. *J. Am. Chem. Soc.* **1955**, *77*, 334.

picture also predicts that for the more endothermic reactions, the ground-state geometries will show the least distortion toward the products, because the mixing between the reactant and the product at this geometry is the smallest, due to the large energy gap. (3) And finally, this picture also leads to the corollary of the Hammond postulate, that the barrier height for an endothermic reaction should be higher than that for a thermoneutral reaction, but that the exothermic reverse reaction should have the lower barrier. In these specific cases, the fragmentations of the cyclopentadiene adducts **5**, **9**, and **11** all relieve more strain than the fragmentations of **13**, **10**, and **12**; this translates into less endothermic reactions overall and thus the lower barrier heights. This correlation between reaction energies and activation energies has been explored before in the context of Diels-Alder reactions.[20]

The most endothermic of the six reactions (**5**, **9**−**13**) is the fragmentation of **12** (28.7 kcal/mol). This reaction has the highest barrier of 46.8 kcal/mol. The transition structure (**12TS**) has the longest partial bonds 2.299 and 2.291 Å, while the ground state of **12** has the shortest bonds *a* and *b*: 1.558 Å (calculated) and 1.552 and 1.552 Å (experimental). Remarkably, all of these results are qualitatively and quantitatively consistent with the Bell−Evans−Polanyi prediction of Figure 3.

The Question of Synchroniety. The Diels-Alder reaction is generally accepted as being a concerted reaction involving a symmetrical transition state with similar degrees of bond formation between the two ends of the diene with the two ends of the dienophile, particularly if both the diene and dienophile are symmetrical.[21] Consequently, the *retro*-Diels-Alder reaction of symmetrical cycloadducts (e.g. as with **5**, **9**, **10**, **11**, and **12** above) would be expected to have similar degrees of bond breaking at the transition state. Indeed the calculated transition states for the *retro*-Diels-Alder reactions of **5** and **9** − **13** (Figure 1, Table 7) are all synchronous. The crystal structures of the cycloadducts **5**, **9**, **10**, **11**, and **12** above all show similar degrees of lengthening of the two C−C bonds which break in this process and thus support the synchronous transition state model. The *retro*-Diels-Alder reaction of a cycloadduct formed from an unsymmetrical diene and/or dienophile would be expected to show an unsymmetrical transition state, with differing degrees of bond breaking of the two C−C bonds.[22] Does this asymmetry manifest itself in the ground state as differing degrees of bond lengthening of the two C−C bonds? The calculated transition state (**15TS**) for cycloreversion of the cycloadduct **15** which is shown in Figure 1 is highly asymmetrical with bond breaking between the methoxy-substituted bridgehead carbon and the quinone moiety being more advanced than at the unsubstituted bridgehead carbon. There is also a net transfer of charge of 0.34 esu (NBO analysis) from the electron-rich diene moiety to the quinone moiety of **15TS**. Comparison of this transition state structure to that calculated for the *retro*-Diels-Alder reaction

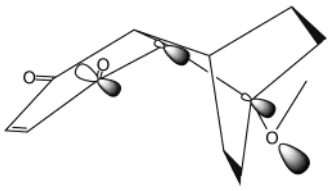

Figure 5.

of the 222 cyclohexadiene cycloadduct **13** reveals that the bond breaking between the methoxy-substituted bridgehead carbon is more advanced while bond breaking at the unsubstituted bridgehead carbon is less advanced than that at the symmetrical cycloadduct.

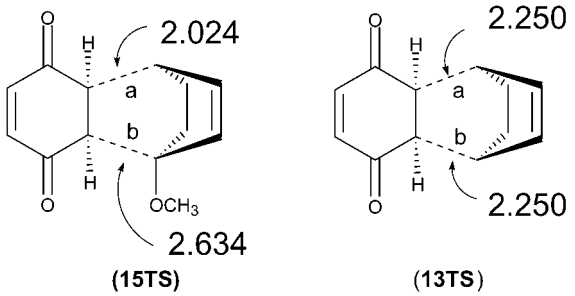

It is very interesting to compare the X-ray structures of the three cycloadducts **13**, **14**, and **15**. In the symmetrical cycloadduct **13** bonds *a* and *b* are 1.571 Å long, whereas in the methoxy-substituted derivative **15** they are 1.587 and 1.556 Å and in the trimethylsiloxy derivative **15** they are 1.585 and 1.563 Å, respectively. The increase in the bond *a* distance in **14** and **15** is unlikely to be due to a steric interaction between the oxygen substituent with the *peri*-disposed carbonyl oxygen, as the two bond distances *a* and *b* are predicted to be the same by molecular mechanics. Clearly the asymmetry in the transition state structure for the rDA reaction in **14** compared with **13** is indeed manifest in the ground-state structure, thus the bond *a* in **14** is longer than the corresponding bond in the symmetrical cycloadduct **13** while bond *b* is shorter.

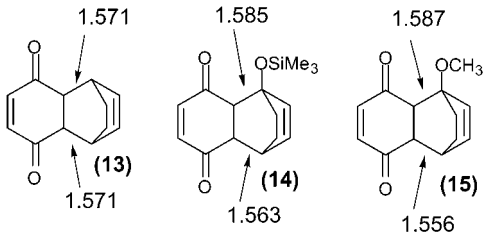

A comparison between the calculated structural parameters for **15** and those observed in the X-ray structure reveals a fairly close agreement in the bond distances, except that bond *a*, which is calculated to be 1.600 Å, is slightly longer than the 1.587 Å that was observed. It is interesting to note that in the calculated structure for the saturated analogue **15s** (Table 6) the bond distances *a* and *b* are 1.584 and 1.553 Å, respectively. The bond *a* is lengthened also in the structure which can no longer undergo the rDA reaction. We believe that the lengthening of bond *a* in **14s** arises from a Grob-like interaction between the methoxy oxygen nonbonded electron pair and the carbonyl π^* orbital via the intervening C−C bond (Figure 5), and represents the manifestation of a *retro*-Aldol reaction in the ground-state structure.

(20) Pilet, O.; Birbaum, J.-L.; Vogel, P. *Helv. Chim. Acta* **1983**, *66*, 19. Vogel, P. *Advances in Theoretically Interesting Molecules*; Thummel, R. P., Ed.; JAI Press: Greenwich, CT, 1989; Vol. 1, pp 201−205.

(21) (a) Tolbert, L. M.; Ali, M. B. *J. Am. Chem. Soc.* **1981**, *103*, 2104. (b) Beno, B. R.; Houk, K. N.; Singleton, D. A. *J. Am. Chem. Soc.* **1996**, *118*, 9984. (c) Houk, K. N.; Li, Y.; Evanseck, J. D. *Angew. Chem., Int. Ed. Engl.* **1992**, *31*, 682. For butadiene plus acrolein, see: (d) Loncharich, R. J.; Brown, F. K.; Houk, K. N. *J. Org. Chem.* **1989**, *54*, 1129. (e) Garcia, J. I.; Martínez-Merino, V.; Mayoral, J. A.; Salvatella, L. *J. Am. Chem. Soc.* **1998**, *120*, 2415. For an argument for asynchronous transition states, see: Dewar, M. J. S. *J. Am. Chem. Soc.* **1984**, *106*, 209.

(22) Gajewski, J. J.; Peterson, K. B.; Kagel, J. R.; Huang, Y. L. *J. Am. Chem. Soc.* **1989**, *111*, 9078.

Scheme 3

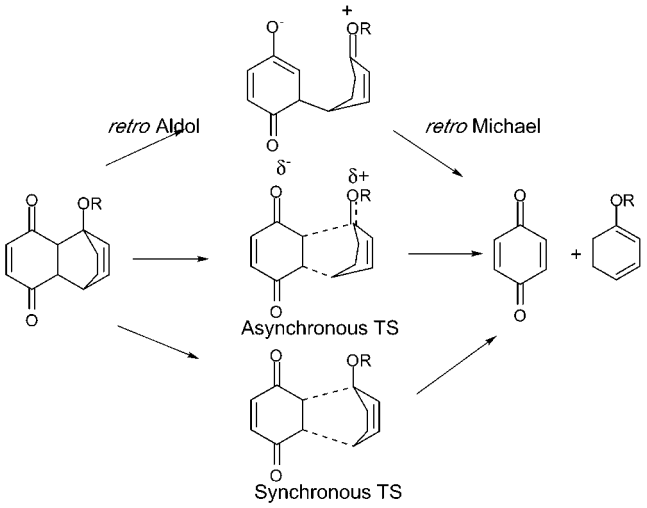

In fact it is compelling to argue that the extra bond lengthening of bond *a* vs bond *b* in the calculated and X-ray crystal structures of **14** and **15** represents the manifestation of both the *retro*-Aldol and *retro*-Diels-Alder reactions in the ground-state structures of **14** and **15**. Perhaps one could go a step further and argue that the *retro*-Diels-Alder reaction of **14** and **15** lies between the extremes of a perfectly synchronous reaction as is predicted to be the case for **13** and a stepwise reaction involving a "pure" *retro*-Aldol reaction as the first step followed by a *retro*-Michael reaction as the second step (Scheme 3 below).

Consistent with this picture is that the calculated transition state structure for **15** has a degree of positive charge of 0.34 esu (NBO analysis) dispersed in the developing diene fragment and negative charge build up dispered in the developing quinone. Consistent with this is the partial "enolic" character of the C1 carbonyl that is evident upon inspection of the geometrical parameters in Table 7, thus the C1−C2 distance is 1.447 Å whereas the C7−C8 distance is 1.500 Å.

Experimental Section

(a) Crystallography. Diffraction data were recorded on an Enraf Nonius CAD4f diffractometer operating in the $\theta/2\theta$ scan mode at low temperature (130.0 K) for all structures. The crystals were flash cooled using an Oxford Cryostream cooling device. Unit cell dimensions were corrected for any θ zero errors by centering reflections at both positive and negative θ angles. The data were corrected for Lorentz and polarization effects.[22] Structures were solved by direct methods (SHELXS-86)[23] and were refined on F^2 (SHELXL-97).[24] Full lists of atomic coordinates, geometrical parameters, and thermal ellipsoid plots for compounds **9**, **9s**, and **10**−**15** have been included in the Supporting Information. Data have been deposited at the Cambridge Crystallographic Data Centre CCDC No. 181481-181489.

(b) Synthesis. Experimental procedures are reported as part of the Supporting Information.

Acknowledgment. Our thanks go to the Australian Research Council and the Robert A. Welch Foundation for financial support.

Supporting Information Available: Experimental details and data (PDF). This material is available free of charge via the Internet at http://pubs.acs.org.

JA025634F

(23) Gable, R. W.; Hoskins, B. F.; Linden, A.; McDonald, I. A. S.; Steen, R. J. *Process_data*, Program for Processing of CAD-4 Diffractometer Data; University of Melbourne: Melbourne, Australia, 1994.
(24) Sheldrick, G. M. *SHELXS-86*, Crystallographic Computing 3.
(25) Sheldrick, G. M. *SHELXL-97*, Program for Crystal Structure Refinement; University of Gottingen: Gottingen, Germany, 1997.